Available online at www.sciencedirect.com
SCIENCE DIRECT
ELSEVIER
Polymer 46 (2005) 5956–5965
polymer
www.elsevier.com/locate/polymer

Morphology and mechanical behavior of isotactic polypropylene (iPP)/syndiotactic polypropylene (sPP) blends and fibers

Xiuqin Zhang[a,c], Ying Zhao[b], Zhigang Wang[a], Chunxiao Zheng[a,c], Xia Dong[b], Zhiqiang Su[b], Peiyu Sun[b], Dujin Wang[a,b,*], Charles C. Han[a,b], Duanfu Xu[b]

[a]*Key Laboratory of Engineering Plastics, Joint Laboratory of Polymer Science and Materials, Institute of Chemistry, Chinese Academy of Sciences, Beijing 100080, China*
[b]*State Key Laboratory of Polymer Physics and Chemistry, Joint Laboratory of Polymer Science and Materials, Institute of Chemistry, Chinese Academy of Sciences, Beijing 100080, China*
[c]*Graduate School of Chinese Academy of Sciences, Beijing 100080, China*

Received 29 December 2004; received in revised form 3 May 2005; accepted 3 May 2005
Available online 22 June 2005

Abstract

The crystallization morphologies and mechanical behaviors of iPP/sPP blends and the corresponding fibers were investigated in the present work. For all the investigated iPP/sPP blends, the starting crystallization temperature of sPP during cooling process was significantly increased with increasing iPP content. The iPP/sPP blends are strongly immiscible at the conventional melt processing temperatures, in consistence with the literature results. As isothermally crystallized at 130 °C, sPP still keeps melt state, while iPP component is able to crystallize and the spherulites become imperfect accompanied by decreasing of the crystallite size as sPP content increases. The addition of sPP decreases the crystallinity of iPP/sPP blends and fibers. The storage modulus, E', of the iPP/sPP blends is higher than that of sPP homopolymer in the temperature range from −90 to 100 °C. The iPP/sPP fibers can be prepared favorably by melt-spinning. As sPP content exceeds 70%, the elastic recovery of the iPP/sPP fibers is approximately equal to that of sPP homopolymer fiber. The drawability of the as-spun fiber of iPP/sPP (50/50) is better than that of sPP fiber, which improves the fiber processing performance and enhances the mechanical properties of the final product. The drawn fiber of sPP presents good elastic behavior within the range of 50% deformation, whereas the elastic property of the iPP/sPP (50/50) fiber slightly decreases, but still much better than that of iPP fiber.

Keywords: iPP/sPP Blends; Fibers; Crystallization

1. Introduction

The application of new metallocene catalysts in recent years has allowed rapid development of polyolefins with a wide range of molecular chain structures, morphologies and related properties, among which syndiotactic polypropylene (sPP), recently obtained with high tacticity, is receiving a great attention owing to its new properties compared to isotactic polypropylene (iPP). The importance lies on its excellent toughness and elastic properties. Previous investigations [1–7] indicated that sPP presents a complex polymorphic behavior, and four crystalline forms have been found so far. The most stable form I and the metastable form II are characterized by chains in s (2/1)2 helical $(t_2g_2)_n$ conformation, packed in orthorhombic unit cells. Other two metastable modifications, form III and form IV, present chains in trans-planar and $(t_6g_2t_2g_2)_n$ helical conformations, respectively. Stretching procedures at room temperature can induce a crystal–crystal phase transition from form I or II to form III [1–4]. This transition is almost completely reversible, which endues with the excellent elasticity of sPP fibers.

Despite its interesting elasticity, sPP has not enjoyed such a commercial success as iPP. Besides the poor ductility [8], relatively low mechanical properties, very complicated polymorphism, slow crystallization rate of sPP is the main disadvantage for processing. For improving the

* Corresponding author. Tel.: +86 010 82616255; fax: +86 010 62559373.
E-mail address: djwang@iccas.ac.cn (D. Wang).

0032-3861/$ - see front matter © 2005 Elsevier Ltd. All rights reserved.
doi:10.1016/j.polymer.2005.05.004

comprehensive properties of sPP and extending its commercial use, many modification techniques have been explored.

A simple modification method is blending sPP with other polymers. Gorrasi [9] studied the transport and mechanical properties of iPP/sPP fibers, showing that the presence of iPP greatly increases the drawability of sPP and it is possible to draw the original film up to DR = 10 (draw ratio) at 110 °C. Thomann [10,11] reported the morphology and phase behavior of iPP/sPP blends, and found that the crystalline morphology of the blends is complex and depends strongly on the thermal history in the melt, the crystallization temperature and blend composition. It can be clearly observed that the blends undergo liquid–liquid phase separation in the melt, which yields iPP in sPP matrix, sPP in iPP matrix or bicontinuous phases for the nearly symmetric blends. Wang [12] studied morphology development during isothermal crystallization for iPP/sPP blends, indicating iPP crystals nucleate sPP crystallization in a 50/50 blend and modify the sPP lamellar spacing. Petermann [13,14] investigated the morphologies and mechanical properties of sPP/HDPE blends. The results indicated that the crystallization rate of sPP increases approximately by a factor of four when blended with 1 wt% of HDPE and of more than ten when blended with 10 wt% of HDPE, and the start crystallization temperature increases more than 10 °C. However, the mechanical properties of sPP/HDPE blends become worse than both HDPE and sPP, for example, within the HDPE concentration range of 10–70 wt%, no necking is observed and the maximum achievable drawing ratio decreases drastically.

Though much work has been done on the morphology and mechanical properties of iPP/sPP blends, focusing on the crystallization properties, compatibility of blends and elastic modulus, investigation on iPP/sPP blend fiber has seldom been reported, especially the fiber property of elastic recovery. In the present work, we studied the crystallization behavior, mechanical and processing properties of iPP/sPP blends, especially the melt spinnability, and the elastic recovery of iPP/sPP fibers at different compositions. The results showed that the addition of iPP influences the crystallization morphology of the iPP/sPP blends, improving the processing performance and the elastic modulus of sPP. The drawability of the as-spun fiber of iPP/sPP blends is significantly improved compared with that of sPP homopolymer. The present result provides us with an alternative to prepare an unconventional elastic fiber of iPP/sPP blends with both high crystallinity and high elastic modulus.

2. Experimental

2.1. Materials

The iPP sample used in this work was prepared by means of chemical degradation [15] from PP2401, a commercial PP brand, supplied by Yansan Petrochemical Company of China. The M_w of the prepared iPP sample is about 1.77×10^5 with polydispersity (M_w/M_n) of 3.86. The sPP sample was supplied by Atofina Company with M_w of 8.59×10^4 and M_w/M_n of 4.10. The microstructure of sPP chains is characterized by ^{13}C NMR and shows a fraction of fully syndiotactic pentad [rrrr] of 80%.

2.2. Blends and fiber preparation

Blends of iPP/sPP (90/10, 70/30, 50/50, 30/70, 10/90 wt%) were prepared through a Haake-RC90 twin-screw extruder with four zones of temperature, ranging from 150 to 190 °C along the barrel of the extruder. All the iPP/sPP blends were submitted to simulated melt-spinning on a modified MFI instrument, in order to qualitatively examine the spinnability and elasticity variation.

Based on above spinnability test, actual melt-spinning experiments for iPP, sPP and 50/50 iPP/sPP blend were carried out on a single-screw melt extruder (diameter = 30 mm, $L/D = 25$) with a spinneret containing 48 orifices, each of 0.35 mm diameter. The extruder was set with five different temperature zones of 200, 220, 230, 225, and 200 °C at the feed, metering, melt-blending, die and spinneret sections, respectively. The as-spun filaments were collected at a take-up speed of 100 m/min, and followed by one-step thermo-drawing of 2–4 times elongation at 100 °C and a subsequent thermo-fixing process at 110 °C.

2.3. DSC measurement

The crystallization behavior of iPP, sPP and iPP/sPP blends was investigated by a MDSC2910 differential scanning calorimeter (DSC, TA Instruments). All operations were performed under nitrogen environment. The samples were heated to 200 °C at a rate of 10 °C/min and held for 10 min to eliminate thermal history, then cooled at a rate of 10 °C/min to room temperature.

The crystallinity of the blends and fibers was calculated based on the DSC data. We assume the heat of fusion (ΔH_m^0) for 100% crystallinity of iPP to be 209 J/g and that of sPP to be 196 J/g, respectively. The formulas to calculate the crystallinity of both PP homopolymer and iPP/sPP blends are as follows:

$$X_{c,iPP} = \Delta H_{m,iPP}/(\Delta H^0_{m,iPP} \times \text{wt\% iPP}),$$

$$X_{c,sPP} = \Delta H_{m,sPP}/(\Delta H^0_{m,sPP} \times \text{wt\% sPP}),$$

$$X_{c,blends} = X_{c,iPP} \times \text{iPP wt\%} + X_{c,sPP} \times \text{sPP wt\%}$$

2.4. Optical microscopy

The samples for optical microscopic study were prepared

by melting the homopolymers or the blends between two cover glasses. The film thickness between the cover glasses was about 40–60 μm. The samples were held for 10 min at 200 °C and then cooled to 130 °C at a rate of 10 °C/min in a LTS350 (Linkam Scientific Instruments) hot stage. Crystallization was monitored by using a Nikon optical microscope with both phase contrast optics and polarized optics.

2.5. Mechanical measurements of the blends and fibers

Storage modulus of the iPP, sPP, and iPP/sPP blends was measured in tensile, as a function of temperature (−90–100 °C), using dynamic mechanical thermal analysis on a Rheometric Scientific V rheometer. The conditions used are listed as follows: heating rate of 5 °C/min, frequency of 1 Hz, sample length, width and thickness of $10\times6\times0.3$ mm^3, and strain of 0.02%.

The simulated-spinning fibers were drawn 2 times at room temperature using a TOM5000 apparatus. The drawn fibers with an initial length (L_0) were stretched up to a length of L_1 (strain 50%), then the tension was released, and the final length (L_2) of the relaxed specimens was measured after 2 min. The elastic recovery is calculated as

$$\varepsilon(\%) = (L_1 - L_2)/(L_1 - L_0)\times 100$$

The stress–strain curves for the as-spun fibers were measured on a tensile testing machine (YG001A) at a falling speed of 60 mm/min.

Stress–strain hysteresis cycles of the drawn fibers were performed on an Instron-5567 dynamometric apparatus at room temperature. The deformation rate is 100 mm/min, and the initial length of the fibers is 100 mm.

The reported values of all the mechanical properties have been averaged over at least five independent measurements.

2.6. FTIR spectroscopy

FTIR spectra measurements for the drawn fibers were performed within the range of 100% deformation. While stretching and relaxing the fibers, the infrared spectra were in situ recorded by using a Bruker EQUINOX 55 spectrometer with 2 cm^{-1} resolution and 32 scans.

2.7. Wide angle X-ray analysis

XRD data between 6 and 36° were collected using a Rigaku D/MAX-RB X-ray diffractometer with Cu Kα radiation at a generator voltage of 40 kV and a generator current of 50 mA. The fibers were crushed into fragments before measurement.

3. Results and discussion

3.1. Crystallization and morphology of iPP/sPP blends

Fig. 1(a) shows DSC scans of iPP/sPP blends with different sPP concentration during heating. It can be seen that individual iPP and sPP melting endotherms can be observed in the blend compositions of 30–90 wt% sPP, indicating that the crystallization of iPP and sPP occurs separately. An exception is iPP/sPP (90/10) blend, for which DSC curve shows only one endotherm peak, implying that the blend might be miscible at this composition. Another possibility is that the crystallinity of sPP in iPP/sPP (90/10) blend is so small that its melting endotherm can not be detected.

DSC cooling scans (Fig. 1(b)) show distinct crystallization exotherms in the blend compositions of 30–70 wt % sPP, which are associated with separate iPP and sPP crystallization. Exotherm peak of sPP is much broader than that of iPP, indicating that the crystallization rate of sPP is relatively slower than that of iPP. The presence of iPP crystals enhances sPP crystallization as evidenced by the higher sPP crystallization temperature in the blend than sPP homopolymer (shift of 10 °C), which might be beneficial to the sPP processing. It should be pointed out that in iPP/sPP (90/10) blend, sPP crystallization exotherm cannot be detected. In iPP/sPP (10/90) blend, iPP crystallization exotherm can neither be detected. These results are possibly

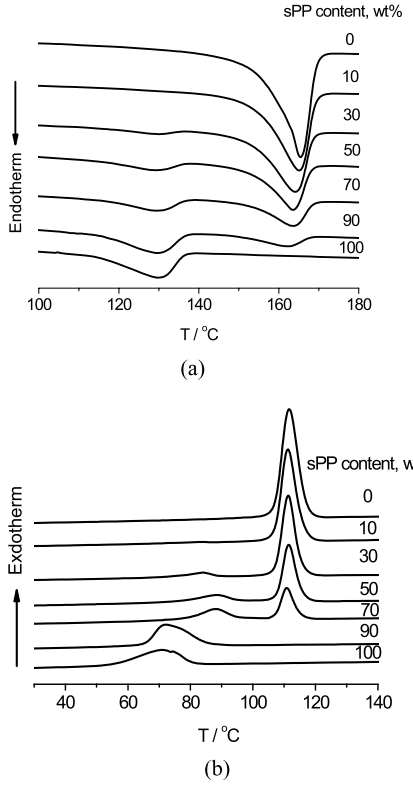

Fig. 1. DSC curves of iPP/sPP blends with different sPP content (wt%): (a) heating scans; (b) cooling scans.

due to low content of sPP (or iPP) or miscibility between iPP and sPP at low composition. Further investigation is undergoing in our laboratory.

Crystallization behavior of sPP has been intensively studied [16–19]. In general, sPP usually appears as needle-like entities, whereas for iPP, spherulites are usually observed. Fig. 2 shows the polarized optical micrographs of iPP and sPP homopolymers crystallized at cooling, forming spherulites for iPP and needle-like crystals for sPP.

In Fig. 3, iPP spherulites can be observed for isothermal crystallization of the blends at low concentrations of sPP (10, 30, 50 wt%). At 130 °C, sPP is in molten state and cannot crystallize, while iPP component is able to grow through the melt with a common nucleation center. However, the presence of sPP influences the growth and size of iPP spherulites. The defects of iPP spherulites increase with increasing sPP content (Fig. 3(a)–(d)). As sPP content exceeds 50 wt%, iPP spherulites are almost unable to be clearly observed (Fig. 3(e)–(f)), indicating the decreasing of the crystal size. At the same time, the crystallinity of the blends decreases with increasing sPP content (Table 1). The small and imperfect crystallites formed in the iPP/sPP blends and the low crystallinity are beneficial to promote the elasticity of iPP/sPP blends.

Fig. 4 shows the phase contrast micrographs of spherulitic macrostructure of iPP homopolymer and phase-separated microdomains of iPP/sPP blends at 130 °C. Spherulitic macrostructure in iPP/sPP (90/10) blend develops a highly nodular, grainy, internal texture. This nodular texture tends to blur spherulitic boundaries, while spherulites can still be seen, which indicates that iPP/sPP (90/10) blend might be partially miscible. With the increase of sPP content (30–50 wt%), spherulitic boundaries are not observed by phase contrast microscope and the coarsening of the phase-separated microdomains increases. This indicates that the iPP/sPP blend pair (sPP content exceeds 10%) might go into the spinodal region. Slow crystallization favors larger scale textures because more time is available for liquid–liquid phase separation (LLPS) until crystallization freezes the morphology. The above observed macromorphology is due to the competition between crystallization and LLPS from an initially well-mixed melt. Because sPP is in melt state and cannot crystallize at 130 °C, iPP/sPP blends are considered to be similar to iPP/aPP blends, whereas the iPP/aPP blends exhibit better miscibility than iPP/sPP blends [20].

Table 1
The crystallinity of iPP/sPP blends (from DSC)

Sample ID	Crystallinity/wt%		
	$X_{c,iPP}$	$X_{c,sPP}$	$X_{c,blends}$
iPP	39.9		
iPP/sPP (90/10)	40.7		36.6
iPP/sPP (70/30)	40.2	4.2	29.4
iPP/sPP (50/50)	40.5	7.4	24.0
iPP/sPP (30/70)	39.8	9.8	18.8
iPP/sPP (10/90)	33.9	11.62	13.8
sPP		15.0	

3.2. Mechanical properties

Fig. 5 shows the temperature dependence of tensile storage modulus, E', of iPP/sPP blends at frequency of 1 Hz. When temperature is lower than −25 °C, E' drops gently for all the samples with a rise in temperature. Within the temperature range from −25 to 0 °C, E' value of sPP decreases rapidly, while E' changes of iPP/sPP blends are much less significant than sPP. Within the whole temperature range of the experiment, E' of the blends is always lower than iPP, except for iPP/sPP (90/10) blend, for which the highest E' values were obtained. This exceptional result might originate from miscibility in iPP/sPP (90/10) blend.

The crystallization results has shown that the addition of sPP (larger than 10 wt%) destroys markedly the iPP spherulites and brings defects in the iPP crystals, decreasing the crystallinity of the blends, leading to the decrease of E' for the iPP/sPP blends. The E' values of the blends are larger than that of pure sPP but lower than that of pure iPP, giving

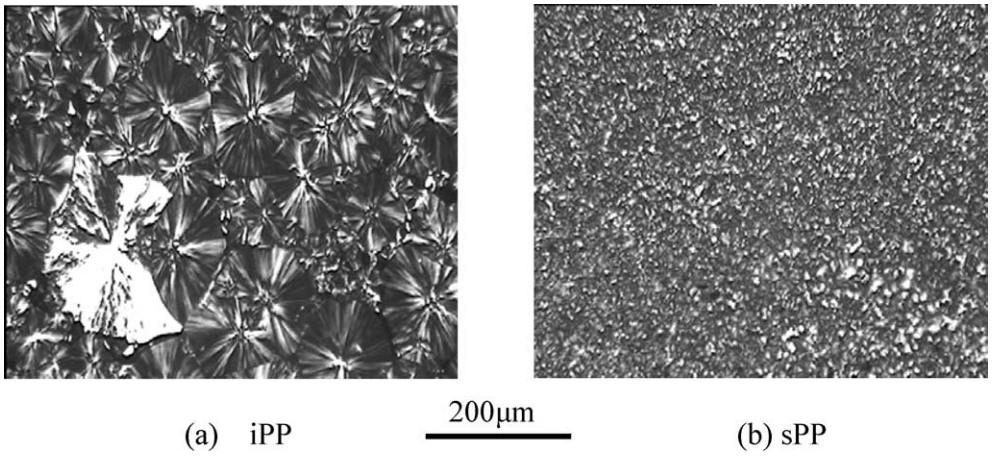

Fig. 2. Polarized optical micrographs of iPP and sPP. Samples were melted at 200 °C for 10 min, and then cooled to room temperature at a rate of 10 °C/min.

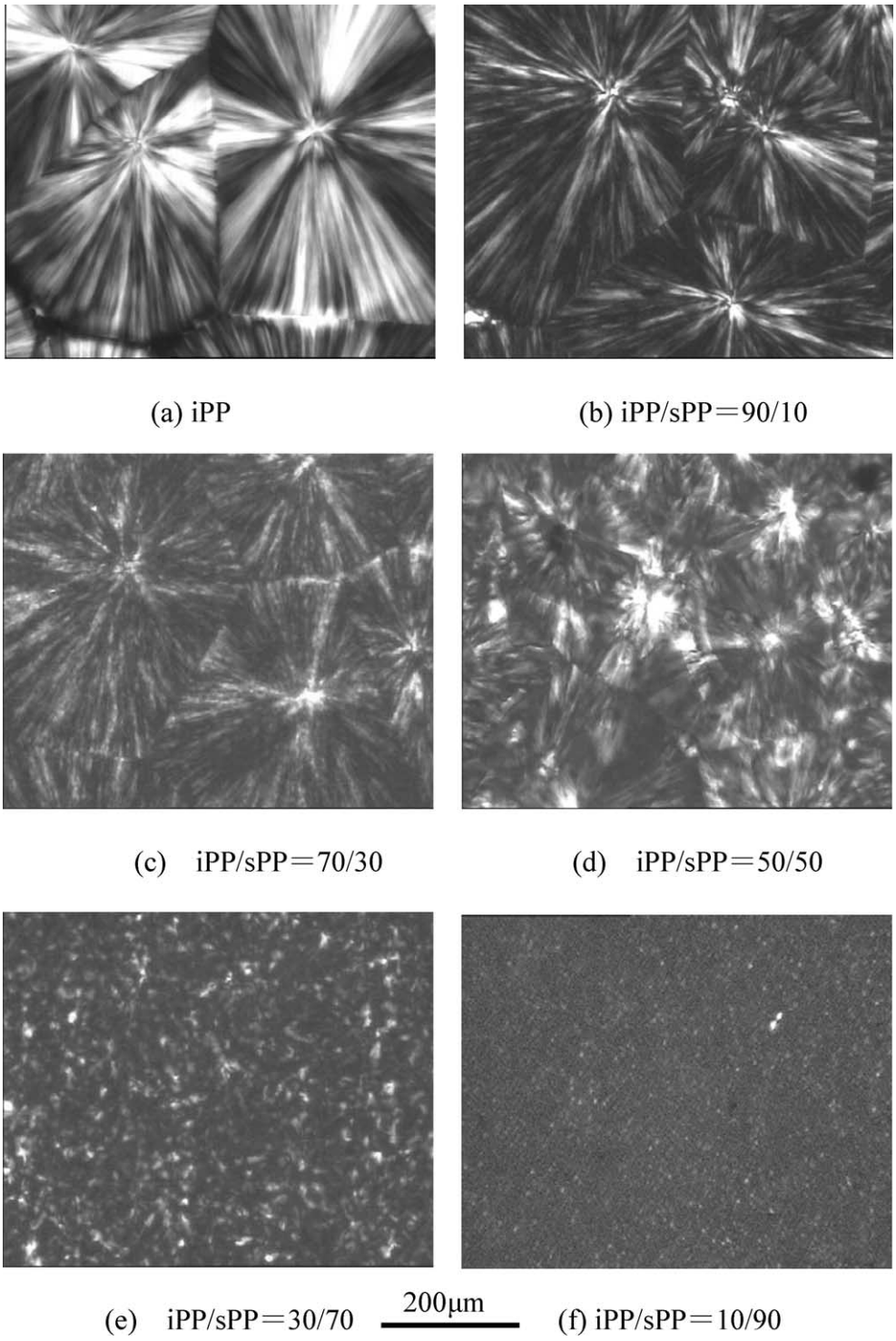

Fig. 3. Polarized optical micrographs of iPP/sPP blends following isothermal crystallization at 130 °C.

a strong indication of partial interconnection of the amorphous phases of both iPP and sPP in the iPP/sPP blends.

As we know, due to slow crystallization rate and poor ductibility, sPP shows poor processing performance [21]. Therefore, in present investigation, iPP was chosen as an additive to improve processing and mechanical properties of sPP, meanwhile excellent elasticity, the intrinsic character of sPP, could be kept at a similar level. Based on the above studies of crystallization and morphology in iPP/sPP blends, the mechanical properties of iPP/sPP fibers were continuously investigated. The simulated melt-spinning on a modified MFI instrument shows that the iPP/sPP blends can be smoothly melt spun into fibers at all the

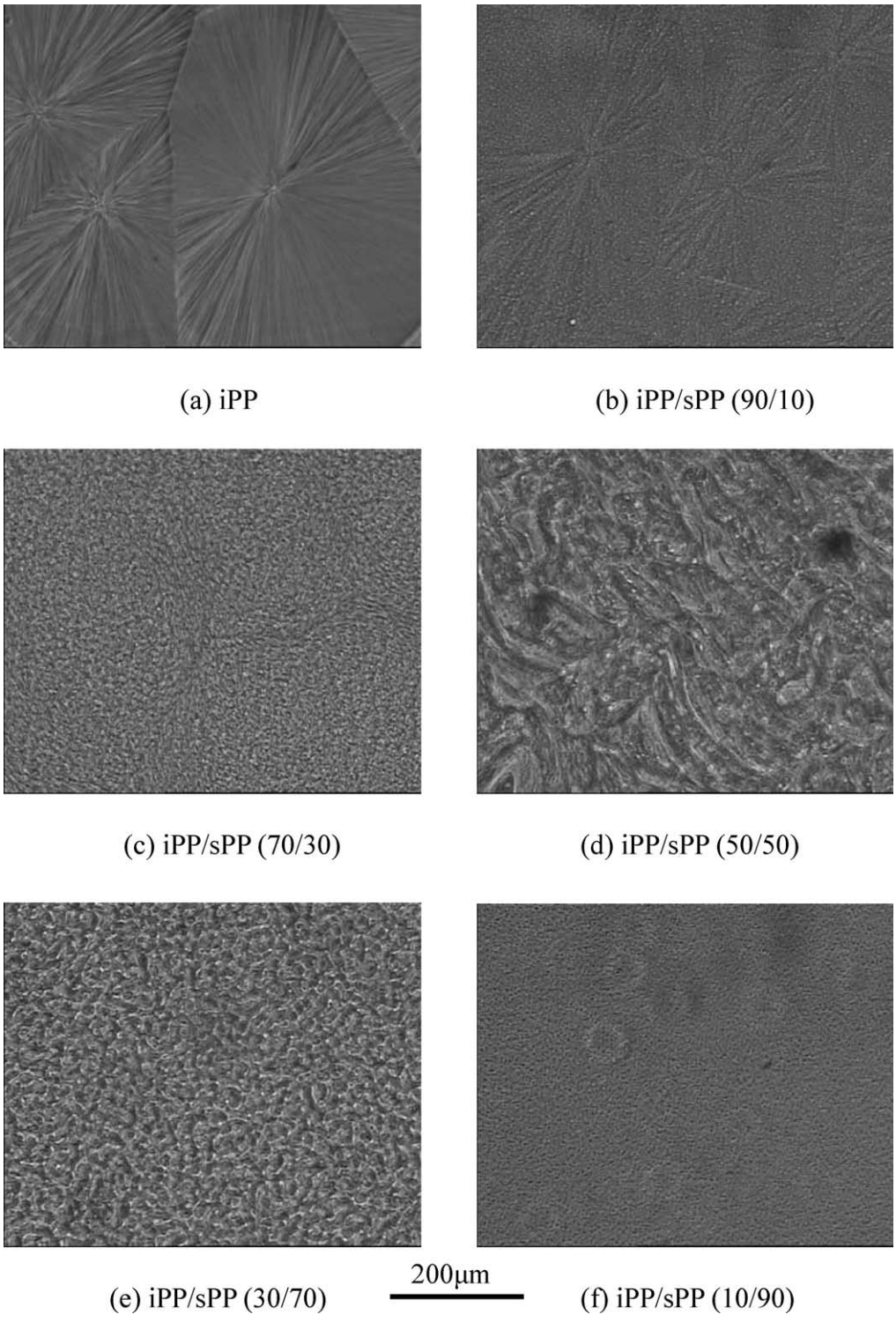

Fig. 4. Phase contrast micrographs of iPP and iPP/sPP blends following isothermal crystallization at 130 °C.

compositions, approving the partial interconnection of the amorphous phases of iPP and sPP. Another reason why phase-separation in the blends does not lead to the break of the fibers might be as follows: as the high temperature melt of iPP/sPP blend was extruded from the spinneret and immediately cooled down to room temperature, the large super-cooling decreased the difference of the crystallization rates of iPP and sPP, thus restraining the phase separation in the blend and improving both the spinnability and elasticity of the iPPP/sPP fibers. The elastic recovery of iPP/sPP fibers is shown in Fig. 6. It is observed that as sPP content exceeds 70 wt%, the elastic recovery of the blended fiber almost

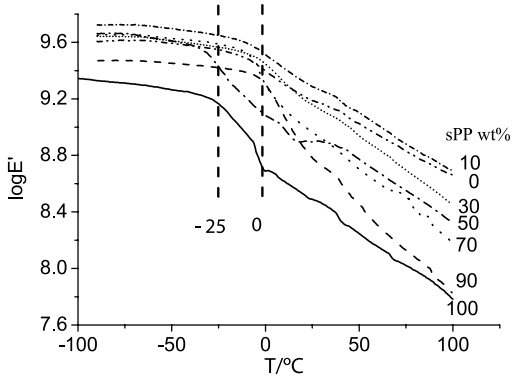

Fig. 5. Logarithm values of tensile storage modulus (E') as a function of temperature for iPP/sPP blends with different sPP content.

keeps constant, approximately equal to that of sPP fiber. As sPP content is lower than 70 wt%, the elastic recovery of the blend fibers decreases rapidly. It should be mentioned that the crystalline structure of iPP also influences the elastic recovery of iPP/sPP fiber, i.e., the small-sized crystals of iPP (shown in Fig. 3(e) and (f)) can act as physical knots of the elastomeric lattice and connect the amorphous phases in iPP and sPP domains. With increasing iPP content, larger spherulites were formed (shown in Fig. 3(a), (b), (c) and (d)) and the crystallinity of the iPP/sPP blends is correspondingly increased (shown in Table 1), resulting in the rapid decrease of the elasticity.

For further understanding the principle of elasticity variation as well as processing performance of iPP/sPP fibers, iPP, sPP and iPP/sPP (50/50) blend were selected for melt spinning. Fig. 7 displays the stress–strain curves of the as-spun fibers. iPP as-spun fiber does not break at testing condition, meaning that its drawability is better than that of sPP and iPP/sPP fibers. The stress–strain curves of sPP and iPP/sPP fibers show usual plastic deformation via necking, which is different from HDPE/sPP blends [14]. No necking has been observed for HDPE/sPP blends, indicating that addition of HDPE is disadvantageous to sPP processing. For iPP/sPP fibers, necking was easily observed, implying that the addition of iPP does not change plastic characteristic of

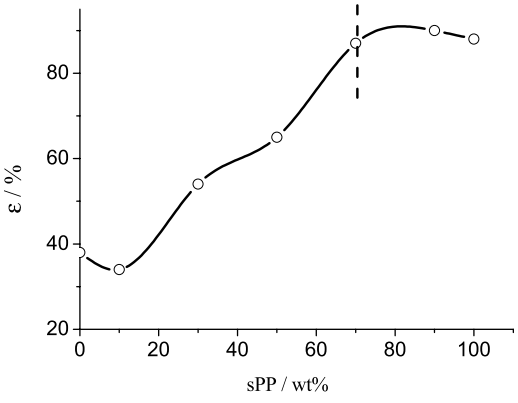

Fig. 6. Elastic recovery of iPP/sPP fibers by simulated melt-spinning on a modified MFI instrument.

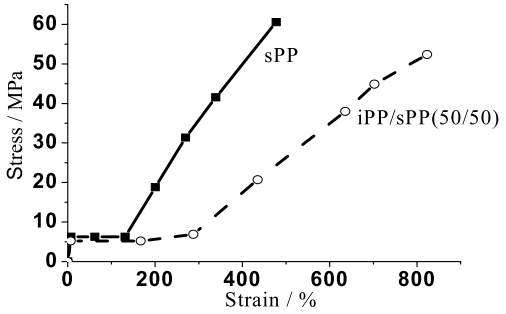

Fig. 7. Stress–strain curves of sPP and iPP/sPP (50/50) as-spun fibers.

sPP. According to Uehara and Gorrasi [8,9], the maximum achievable DR of sPP is ca. 5–7, significantly lower than that of iPP. Poor ductility of sPP has been ascribed to the absence of the crystalline relaxation, which has instead been clearly observed in the highly drawn iPP. The drawability of iPP/sPP (50/50) fiber is much better than that of sPP fiber, which will be certainly beneficial to post-processing of iPP/sPP fibers. The drawability of the blended fibers also means good continuity between the crystalline phase and the connected amorphous matrix.

As-spun sPP fiber can be processed favorably at DR of 2. Increasing DR from 2 to 4, sPP fiber is easy to break. iPP/sPP as-spun fiber, however, can still be drawn as DR is larger than 4. High draw ratio can enhance orientation of the macromolecular chains, greatly improving mechanical properties, which is highly desirable.

To quantify the elastic properties of sPP, iPP and iPP/sPP fibers, hysteresis cycles (Fig. 8) and elastic recovery of multiple stress–strain cycles (Fig. 9) have been performed on the dawn fibers at room temperature. The area of each hysteresis curve represents the energy dissipation during the cycle. The results indicate that the energy dissipation and the permanent set of sPP are lower than that of iPP/sPP fiber and iPP fiber. The elastic recovery of sPP, iPP/sPP and iPP drawn fibers at the fourth cycle is 66, 54 and 30%, respectively, indicating that sPP fiber presents good elastic behavior within 50% deformation, whereas elastic property of iPP/sPP fiber takes the second place, and iPP fiber takes the third place. The difference between elastic behaviors of

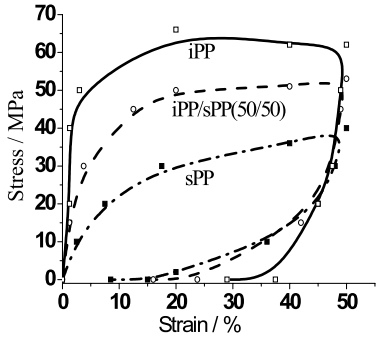

Fig. 8. Stress–strain hysteresis cycles performed for the drawn fibers.

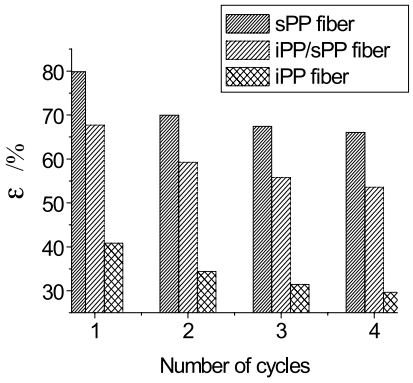

Fig. 9. Elastic recovery of the drawn fibers at different cycles.

different fibers is related to the bulk properties of the materials.

3.3. FTIR spectroscopic investigation on fiber deformation

Conventional thermoplastic elastomers include poorly crystalline or amorphous polymers with glass transition temperatures much lower than room temperature, which partially crystallize under stretching. Small amount of crystals act as knots of the elastomeric network. Those chains, belonging to the amorphous phase and connect crystalline regions as tie chains, experience reversible conformation transition between disordered (coils) and extended conformation when repeatedly stretched and relaxed. The entropic factor is involved in the recovery process. Because of higher crystallinity and glass transition temperature of sPP than conventional elastomers, excellent elasticity of sPP cannot be explained only by the entropic factor. It was found [1,2] that sPP has complex polymorphism, such as form I or II of t_2g_2 conformation, and form III of planar zigzag conformation. Melt-spun sPP fiber exhibits Form I helical structure at low spinning speeds and Form III trans-planar structure at high spinning speeds [22,23]. The crystal structure of the sPP fiber prepared by the spinning speed of 100 m/min should be the form I. Therefore, a reversible crystal–crystal phase transition may occur during stretching and relaxing. In FTIR spectra, the peaks at wavenumbers of 812, 842, 977, 1005, and 1264 cm^{-1} are assigned to form I or II with t_2g_2 helical conformation, and the peaks at wavenumbers of 829, 963, 1130 and 1230 cm^{-1} are assigned to planar zigzag conformation, form III [24]. A parameter commonly used to measure the overall relative helical-to-planar ratio of sPP is the absorbance ratio $R(A_{977}/A_{963})$. Partial FTIR spectra and the values of $R(A_{977}/A_{963})$ of sPP fiber during stretching and relaxing are given in Figs. 10 and 11, respectively. During stretching, relative intensity of the peak at 977 cm^{-1} and $R(A_{977}/A_{963})$ value decrease, while relative intensity of the peak at 963 cm^{-1} increases with increasing strain, indicating that relative amount of helical conformation decreases, while that of trans-planar conformation increases with increasing deformation. The

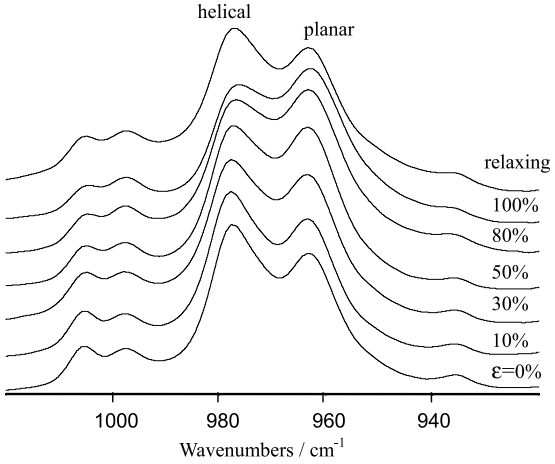

Fig. 10. In situ FTIR spectra of sPP drawn fiber during the courses of stretching and relaxing.

structural changes during stretching are reversible. It can be seen that relative intensity of the peak at 977 cm^{-1} and $R(A_{977}/A_{963})$ value increase for the relaxed sPP fiber, meaning that trans-planar conformation transforms to helical conformation as the applied tension is released. The crystal–crystal transition has also been confirmed by wide-angle X-ray diffraction [1–4,21]. Structural transition occurring in the crystalline region produces an enthalpy gain when tension is released, which together with the entropic factor of amorphous region are responsible for elastic recovery of sPP fibers.

Fig. 12 shows partial FTIR spectra of iPP/sPP (50/50) fibers during stretching and relaxing. Though elasticity of iPP/sPP (50/50) fiber improves compared with iPP (Fig. 9), the spectra do not show obvious changes for the conformation structure during stretching and relaxing, implying that structural transition may not occur or could not be detected by FTIR. This phenomenon might be attributed to the existence of helical conformation of iPP, which confines the conformational transition between helix and trans-planar structures of sPP. Due to the lacking of conformational transition as pure sPP fiber, elastic recovery of iPP/sPP (50/50) fiber decreases, compared with that of sPP fiber. On the other hand, the addition of sPP decreases crystallinity of

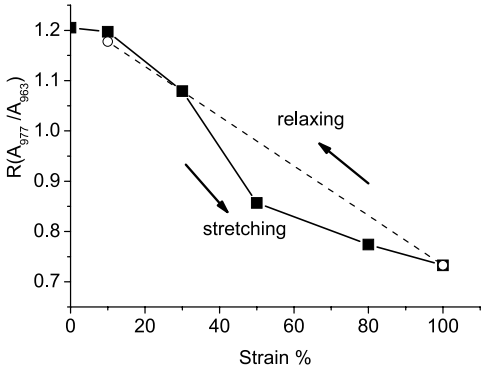

Fig. 11. Absorbance ratio $R(A_{977}/A_{963})$ of sPP as a function of strain.

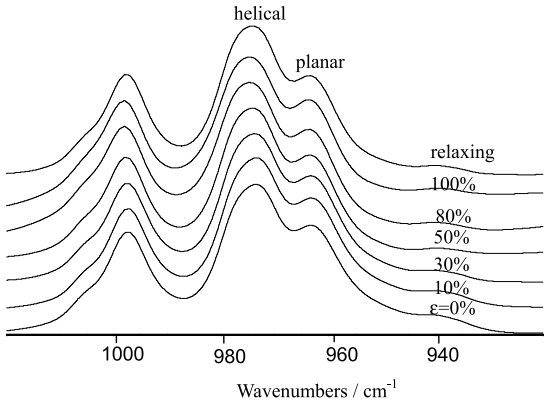

Fig. 12. In situ FTIR spectra of iPP/sPP (50/50) drawn fiber during the courses of stretching and relaxing.

blended fiber (Fig. 13 and Table 2), resulting in an increase of entropic variation in amorphous region. This can lead to elasticity increase of iPP/sPP fiber.

4. Conclusions

The crystallization morphology and mechanical properties of iPP/sPP blends and the elasticity of the corresponding fibers have been investigated. The main conclusions were summarized as follows:

(1) The starting crystallization temperature of sPP increases more than 10 °C if iPP is present, which reflects the favorable nucleation of iPP in the blends. The iPP/sPP blends are strongly immiscible in the crystalline domains but partially interconnected in the amorphous phase, and phase separation develops prior to isothermal crystallization at 130 °C. Defects of the iPP spherulites increase with increasing sPP concentration. When the sPP concentration is larger than 50 wt%, iPP spherulites cannot be clearly observed. The addition of sPP decreases the crystallinity of the iPP/sPP blends and fibers.

(2) Within the experimental temperature range (−90 –100 °C), the E' of iPP/sPP blends is higher than that of sPP. When the content of sPP is larger than 70%, the elastic recovery of iPP/sPP fiber is approximately equal to that of sPP.

(3) sPP and iPP/sPP (50/50) as-spun fibers show usual necking plastic deformation. The drawability of iPP/sPP (50/50) fiber is better than that of sPP fiber, which is beneficial to further processing.

(4) The drawn fibers of sPP and iPP/sPP present good elastic behavior within the range of 50% deformation. The better elasticity of sPP drawn fiber is attributed to the enthalpy gain in the crystalline region, which comes from a reversible crystal–crystal phase transition in the courses of stretching and relaxing, and the entropic variation in the amorphous region. Above two factors may simultaneously act on sPP and mutually assist to each other. The improvement of the elasticity of iPP/sPP (50/50) fiber, however, is mainly due to the entropic variation in the amorphous region.

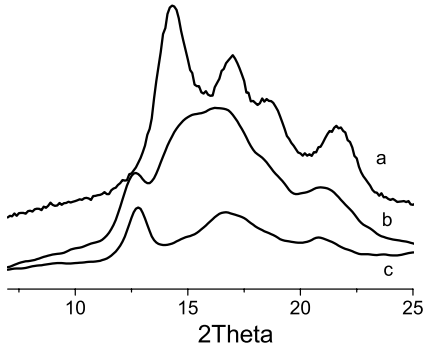

Fig. 13. WAXD patterns of drawn fibers. (a) iPP, (b) iPP/sPP (50/50), and (c) sPP.

Table 2
The crystallinity of iPP/sPP fibers (from DSC)

Sample ID	Crystallinity/%		
	$X_{c,iPP}$	$X_{c,sPP}$	$X_{c,blends}$
iPP	39.3		
iPP/sPP (50/50)	41.5	9.2	25.4
sPP		14.5	

Acknowledgements

This work was supported by National Natural Science Foundation of China (NSFC, grant No. 50290090, 20490220). ZW acknowledges the financial support from 'One Hundred Young Talents' of the Chinese Academy of Sciences, People's Republic China.

References

[1] De Rosa C, Gargiulo MC, Auriemma F, De Ballesteros OR, Razavi A. Macromolecules 2002;35:9083.
[2] Auriemma F, De Rosa C. J Am Chem Soc 2003;125:13143.
[3] Guadagno L, D'Aniello C, Naddeo C, Vittoria V. Macromolecules 2002;35:3921.
[4] Auriemma F, De Ballesteros OR, De Rosa C. Macromolecules 2001; 34:4485.
[5] Ohira Y, Horii F. Macromolecules 2000;33:5566.
[6] Guadagno L, D'Aniello C, Naddeo C, Vittoria V. Macromolecules 2000;33:6023.
[7] Guadagno L, D'Aniello C, Naddeo C, Vittoria V. Macromolecules 2001;34:2512.
[8] Uehara H, Yamazaki Y, Kanamoto T. Polymer 1996;37:57.
[9] Gorrasi G, Vittoria V, Longo P. J Appl Polym Sci 2001;80:539.
[10] Thomann R, Kressler J, Setz S, Wang C, Mülhaupt R. Polymer 1996; 37:2627.
[11] Thomann R, Kressler J, Rudolf B, Mülhaupt R. Polymer 1996;37: 2635.

[12] Wang ZG, Phillips RA, Hsiao BS. J Polym Sci: Part B: Polym Phys 2001;39:1876.
[13] Bonnet M, Loos J, Petermann J. Colloid Polym Sci 1998;276:524.
[14] Loos J, Bonnet M, Petermann J. Polymer 2000;41:351.
[15] Marisa CGR, Fernanda MBC, Stephen TB. Polym Test 1995;14:369.
[16] Wang ZG, Wang XH, Hsiao BS, Phillips RA, Medellin-Rodriguez FJ, Srinivas S, et al. J Polym Sci: Part B: Polym Phys 2001;39:2982.
[17] Loos J, Petermann J. Polymer 1996;7:417.
[18] Andrew JL, Bernard L, Don DD, Martina S. Macromolecules 1994; 27:6603.
[19] Thomann R, Wang C, Kressler J, Jüngling S, Mülhaupt R. Polymer 1995;36:3795.
[20] Phillips RA. J Polym Sci: Part B: Polym Phys 2000;38:1947.
[21] De Rosa C, Auriemma F, Ballesteros OR. Macromolecules 2003;36: 7607.
[22] Sura RK, Desai P, Abhiraman AS. J Appl Polym Sci 2001;81:2305.
[23] Choi D, White J. Polym Eng Sci 2004;44:210.
[24] Nakaoki T, Yamanaka T, Ohira Y, Horii F. Macromolecules 2000;33: 2718.